Interpreting Stationary Wave Nonlinearity in Barotropic Dynamics

LEI WANG AND PAUL J. KUSHNER

Department of Physics, University of Toronto, Toronto, Ontario, Canada

(Manuscript received 24 September 2009, in final form 12 February 2010)

ABSTRACT

Stationary wave nonlinearity describes the self-interaction of stationary waves and is important in maintaining the zonally asymmetric atmospheric general circulation. However, the dynamics of stationary wave nonlinearity, which is often calculated explicitly in stationary wave models, is not well understood. Stationary wave nonlinearity is examined here in the simplified setting of the response to localized topographic forcing in quasigeostrophic barotropic dynamics in the presence and absence of transient eddies. It is shown that stationary wave nonlinearity accounts for most of the difference between the linear and full nonlinear response, particularly if the adjustment of the zonal-mean flow to the stationary waves is taken into account. The separate impact of transient eddy forcing is also quantified. Wave activity analysis shows that stationary wave nonlinearity in this setting is associated with Rossby wave critical layer reflection. A nonlinear stationary wave model, similar to those used in baroclinic stationary wave model studies, is also tested and is shown to capture the basic features of the full nonlinear stationary wave solution.

1. Introduction

The stationary wave field, which is the zonally asymmetric part of the time mean flow, is a principal field to explain in the atmospheric general circulation. It plays a significant role in the eddy-driven zonal mean circulation and is key to understanding climate variability and change on regional scales (e.g., Held et al. 2002, and references therein). Stationary wave theory has progressed from a focus on the simple linear response to thermal and orographic forcing (e.g., Hoskins and Karoly 1981) to a quantitative framework that accounts for nonlinear stationary wave effects, transient eddy effects, and sensitivity to the zonal mean flow (e.g., Valdes and Hoskins 1991; Ting and Yu 1998; Joseph et al. 2004; Brandefelt and Körnich 2008; Chang 2009). This development has been based on stationary wave models that solve for the stationary wave field in the presence of prescribed zonal mean and zonally asymmetric forcing fields; the prescribed fields are understood to fall outside the stationary wave theory itself.

In this study we focus on the so-called ''stationary wave nonlinearity,'' also known as ''stationary nonlinearity'' or ''nonlinear self-interaction,'' which arises primarily through advective terms in the equations of motion and becomes more important for larger-amplitude stationary waves (e.g., Ting et al. 2001, and references therein). For example, in quasigeostrophic (QG) dynamics, stationary wave nonlinearity involves the flux of stationary eddy potential vorticity (PV) by the stationary eddy velocity. Observed stationary wave amplitudes are sufficiently large that stationary wave nonlinearity is a leading-order term in stationary wave dynamics, comparable in impact to topographic forcing (Valdes and Hoskins 1991; Ting 1994; Ting et al. 2001). Classically, linear stationary wave models have diagnosed the importance of stationary wave nonlinearity by imposing the stationary wave nonlinearity as an external forcing (e.g., Ting 1994). But nonlinear techniques have also been developed that predict the stationary wave nonlinearity as part of a stationary wave calculation (Valdes and Hoskins 1991; Jin and Hoskins 1995; Ringler and Cook 1997; Ting and Yu 1998; Held et al. 2002).

Our aim in this study is to improve our dynamical understanding of stationary wave nonlinearity and to evaluate the nonlinear stationary wave modeling technique of Ting and Yu (1998) and Held et al. (2002). We do so in the classical setting of barotropic QG dynamics on the sphere, in which we will see that stationary wave nonlinear effects primarily involve stationary Rossby wave reflection at critical latitudes (Nigam and Held

Corresponding author address: Lei Wang, Department of Physics, University of Toronto, 60 St. George St., Toronto, ON M5S 1A7, Canada.
E-mail: lei@atmosp.physics.utoronto.ca

DOI: 10.1175/2010JAS3332.1

1983; Held and Phillips 1987). We here consider in detail the regional response to isolated forcing in the presence and absence of transient eddies. We separately consider the nonlinear effects of stationary and transient eddies in the zonal mean and zonally asymmetric flow. Understanding this elementary model problem is, in our view, a necessary step to understanding the baroclinic nonlinear stationary wave calculations of Ting and Yu (1998) and Held et al. (2002), which we are currently applying to the study of the three-dimensional stationary wave response to climate change. To our knowledge, our results concerning zonally asymmetric stationary wave nonlinearity in the presence and absence of transient eddies, applied to this simple system, have not previously been documented.

After describing the set of dynamical equations and techniques we use (section 2), we analyze a strongly damped case in which transient eddies are absent and in which the only nonlinearity arises from the stationary wave field itself (section 3). We also develop a weakly nonlinear asymptotic theory to explicitly account for the stationary wave nonlinear effects. We then examine a more weakly damped case in which transient eddies are important and test a Ting–Yu type nonlinear stationary wave model that numerically predicts the stationary wave nonlinearity. In both the strongly damped and weakly damped cases, critical-layer reflection is important, but in the weakly damped case the adjustment of the zonal mean basic state also needs to be accounted for to accurately reproduce the critical-layer reflection. Conclusions are presented in section 4.

TABLE 1. Variable notations and definitions.

Notation	Definition
ζ	Vorticity
ψ	Streamfunction
τ_Z	Damping time scale for zonal mean flow
τ_E	Damping time scale for eddies
[ ]	Zonal mean
$\bar{}$	Time mean
*	Deviation from zonal mean
′	Deviation from time mean
U	Prescribed time-independent and zonally symmetric zonal wind
Z, Z_0	Prescribed time-independent and zonally symmetric vorticity and its representative value (1×10^{-5} s^{-1})
$\mathbf{u}$	Horizontal velocity, $\mathbf{u} = (u, v)$, zonal and meridional winds, respectively
f, f_0	Coriolis parameter and its representative value (1×10^{-4} s^{-1})
ν	Resolution-dependent hyperdiffusion coefficient; $\nu = 2.7 \times 10^{50}$ m^8 s^{-1} for the highest meridional mode with zero zonal mode in T85, corresponding to a 3-h damping time scale on this mode
ζ_{ref}	Vorticity of a zonally symmetric reference zonal flow corresponding to $U_{\text{ref}} = 25\cos\theta - 30\cos^3\theta + 300\sin^2\theta\cos^6\theta$ (Held 1985)
h	Topography, a Gaussian mountain centered at (λ_0, θ_0) with half-width $\Delta\lambda$ and $\Delta\theta$; $h = h_0 \exp\{-(\lambda-\lambda_0)^2/(\Delta\lambda)^2 - (\theta-\theta_0)^2/(\Delta\theta)^2\}$, where $\lambda_0 = 90°$, $\theta_0 = 30°$, $\Delta\lambda = \Delta\theta = 22.5°$, $h^* = h - [h]$

2. Numerical models and diagnostics

We consider barotropic vorticity dynamics on a rotating sphere in the presence of relaxation to a prescribed zonal flow that represents the boreal winter upper tropospheric wind, and in the presence of orography that generates a Rossby lee wave train. We first solve by direct nonlinear simulation (DNS) the equation

$$\frac{\partial\zeta}{\partial t} + \nabla\cdot\left\{\left(f+\zeta+\frac{f_0 h}{H}\right)\mathbf{u}\right\} + \frac{1}{\tau_Z}([\zeta]-\zeta_{\text{ref}}) + \frac{1}{\tau_E}\zeta^* + \nu\nabla^8\zeta = 0, \quad (1)$$

where the notation, which is for the most part standard, is described in Table 1. We solve (1) using a T85 (1.4°) resolution pseudospectral model from the National Oceanic and Atmospheric Administration/Geophysical Fluid Dynamics Laboratory Flexible Modeling System. The zonal asymmetry in the model arises from a mountain whose amplitude is determined by h_0; the amplitude of the associated potential vorticity perturbation is $(h_0/H)f_0$, where $H = 10$ km is a representative depth for the troposphere. Standard QG scaling (Vallis 2006) requires that the PV contribution from topography be comparable to ζ; that is, $f_0 h/H \sim f_0 h_0/H \sim \zeta \sim Z_0$, where ζ and Z_0, from Table 1, provide scales for the vorticity and topography. We define a topographic amplitude parameter $\varepsilon = f_0 h_0/Z_0 H$. For linear theory to be applicable, the PV contribution from topography needs to be small compared to ζ (i.e., $\varepsilon \ll 1$). We test cases in the range $100\text{ m} \le h_0 \le 2$ km, which corresponds to $0.1 \le \varepsilon \le 2$. In section 3c, we develop diagnostics based a small-parameter expansion of the equations in ε.

The response of a given field to this topography is defined as the solution with topography minus the solution without topography. In the absence of topography, the solution has the zonal jet given by U_{ref}, slightly spread out by hyperviscosity, and U_{ref} is taken as the basic background flow.

We consider two cases in this study. In the strongly damped (SD) case, we set $\tau_Z = \tau_E = 5$ days, which provides sufficiently strong damping to suppress transient eddies that arise because of the instability of the zonally asymmetric flow. The SD case represents a classical application of this model to the stationary wave problem

and is useful for testing ideas. In the weakly damped (WD) case, we set $\tau_Z = 5$ days and $\tau_E = \infty$, which allows transient waves and a transient zonal flow to develop. The WD case is qualitatively more realistic and perhaps more relevant to the observed general circulation, but it is much more complex because of transient eddy effects.

The time average of (1) has zonal mean component

$$\nabla \cdot \left\{ \left[\left(\overline{\zeta}^* + \frac{f_0 h^*}{H} \right) \overline{\mathbf{u}}^* \right] + [\overline{\zeta' \mathbf{u}'}] \right\} + \frac{1}{\tau_Z}([\overline{\zeta}] - \zeta_{\text{ref}}) = 0, \tag{2}$$

and zonally asymmetric component

$$\nabla \cdot \left\langle \left(f + [\overline{\zeta}] + \frac{f_0[h]}{H} \right) \overline{\mathbf{u}}^* + \left(\overline{\zeta}^* + \frac{f_0 h^*}{H} \right) [\overline{\mathbf{u}}] + \left\{ \left(\overline{\zeta}^* + \frac{f_0 h^*}{H} \right) \overline{\mathbf{u}}^* + \overline{\zeta' \mathbf{u}'} \right\}^* \right\rangle + \frac{1}{\tau_E} \overline{\zeta}^* = 0, \tag{3}$$

where we have not included the (relatively small) hyperviscous term. In the SD case, the transient eddy vorticity flux $\overline{\zeta' \mathbf{u}'} = 0$, and these two equations represent a closed system that could in principle be solved for the zonally symmetric and the zonally asymmetric components of the flow. In practice, we use prognostic versions of these equations, along the lines of (4) below, to solve for these components of the flow. In the more realistic WD case, $\overline{\zeta' \mathbf{u}'} \neq 0$, and in the absence of an accurate mean flow parameterization of the transient eddy fluxes, we must integrate (1) by DNS and take its time average to get the stationary wave field. In particular, we show the day 200–1000 average fields in the WD case.

In contrast to (2) and (3), stationary wave models represent so-called "anomaly models" in which only the stationary wave terms of the general form $\overline{A}^*$ for a field A are solved for and other fields are prescribed as consistently as possible with the original equations. We consider two types of stationary wave model in this study. The linear stationary wave model (LIN-ANOM) integrates to a steady state the equation

$$\frac{\partial \zeta^*}{\partial t} + U \frac{\partial \left(\zeta^* + \frac{f_0 h^*}{H} \right)}{a \cos\theta \partial\lambda} + v^* \frac{\partial \left(f + Z + \frac{f_0[h]}{H} \right)}{a \partial\theta} + \frac{1}{\tau_E} \zeta^* = F^*, \tag{4}$$

which is linear in the zonally asymmetric terms like ζ^*. The right-hand term F^* is a prescribed "forcing" that represents the zonally asymmetric component of the eddy vorticity flux convergence and can include either or both of the stationary and transient eddy contributions to this flux taken from the DNS solution of (1). The terms U, Z, and F^* are not genuine external forcing but rather inherently dynamical quantities that are treated as forcing for diagnostic purposes. In addition, τ_E, which is used in the linear model, is a tuning parameter to stabilize the solution as necessary.

The second anomaly model we consider is a nonlinear stationary wave model (NONLIN-ANOM) in which we integrate

$$\frac{\partial \zeta^*}{\partial t} + U \frac{\partial \left(\zeta^* + \frac{f_0 h^*}{H} \right)}{a \cos\theta \partial\lambda} + v^* \frac{\partial \left(f + Z + \frac{f_0[h]}{H} \right)}{a \partial\theta} + \nabla \cdot \left\{ \left(\zeta^* + \frac{f_0 h^*}{H} \right) \mathbf{u}^* \right\}^* + \frac{1}{\tau_E} \zeta^* = F^* \tag{5}$$

to a "quasi-steady" state, by which we mean that transients are suppressed to the extent that it is practicable while maintaining a reasonable solution (similar to Held et al. 2002; see section 3e). This equation corresponds to the Ting and Yu (1998) and Held et al. (2002) nonlinear baroclinic stationary wave model, whose performance we wish to evaluate in this simplified setting of barotropic dynamics. In this model, the zonal mean flow is again prescribed via U and Z, but now F^* is understood to represent only the transient eddy contribution. In this model, τ_E is again set to a minimum value that stabilizes the flow.

A final anomaly model we use is a prognostic version of the zonal mean equation (2) to diagnose the zonal mean state in the presence of prescribed time averaged zonal mean eddy vorticity flux convergence of either or both of the stationary and transient eddies (ZONAL-ANOM). This calculation is a barotropic version of classical baroclinic calculations of the zonal mean circulation consistent with a prescribed eddy forcing, which is commonly known as the "downward control" diagnostic in the stratospheric literature (Haynes et al. 1991).

To diagnose the wave response we show three principal diagnostics. First, we display the zonally asymmetric streamfunction ψ^*. Second, we plot the propagation of Rossby wave activity in the longitude–latitude plane using the Plumb (1985) wave activity flux, which for barotropic flow linearized about a zonally symmetric basic state reduces to

$$\mathbf{W} = \frac{\cos\phi}{2} \left(v^{*2} - \frac{\psi^*}{a \cos\phi} \frac{\partial v^*}{\partial \lambda}, -u^* v^* - \frac{\psi^*}{a} \frac{\partial v^*}{\partial \phi} \right).$$

This wave activity flux is parallel to the local group velocity of stationary Rossby waves in the Wentzel–Kramers–Brillouin (WKB) limit for monochromatic

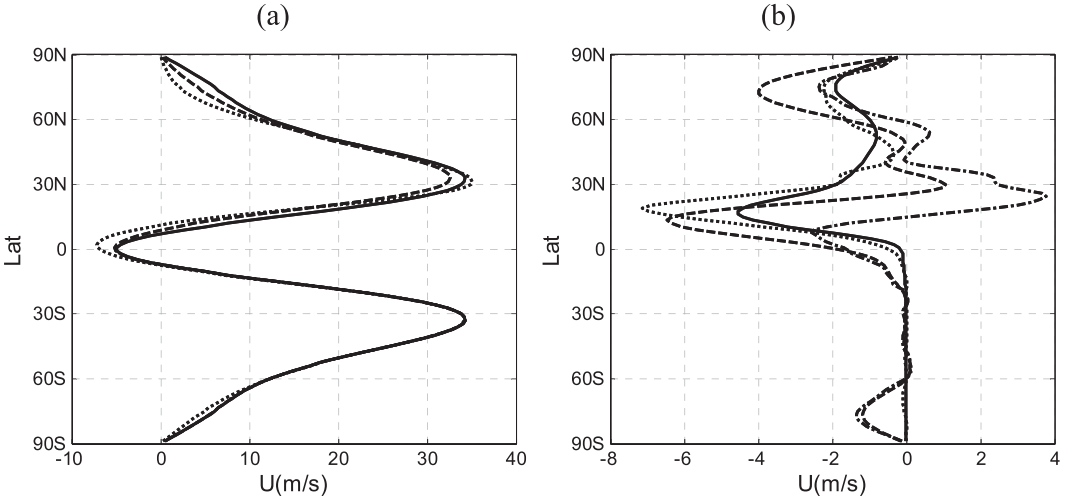

FIG. 1. (a) For $\varepsilon = 2$, U_{ref} (solid), $[u]_{\text{SD}}$ (dashed), and $[u]_{\text{WD}}$ (dotted). (b) SD zonal wind response (solid), WD zonal wind response (dashed), WD response to stationary eddy forcing (dotted), and WD response to transient eddy forcing (dashed–dotted). Units are meters per second.

waves, but it has also been found useful for wave pockets that are more relevant in this study. Finally, we make use of Taylor (2001) diagrams that combine information about the correlation and relative magnitude of two fields as a single point in a polar-coordinate plane; this allows us to concisely represent the results of several sensitivity tests.

3. Results

a. Zonal wind response

Figure 1a shows U_{ref}, the SD case zonal wind $[u]_{\text{SD}}$, and the WD case zonal wind $[u]_{\text{WD}}$ for a mountain with $h_0 = 2$ km. The Northern Hemisphere jet is slowed down by the mountain in the SD case but is sharpened (with acceleration of the maximum and deceleration of the flanks) in the WD case. In Fig. 1b, we show the zonal wind response for the SD case, which is almost entirely associated with the stationary eddy forcing, with a much weaker contribution from hyperdiffusion. We also show the WD response and the decomposition of the WD response into parts associated with the zonally symmetric components of the stationary eddy vorticity flux and of the transient eddy vorticity flux, using the ZONAL-ANOM model as discussed in section 2. We see that the stationary wave vorticity flux has a similar decelerating effect in the SD and WD cases, but that the transient eddy vorticity flux in the WD case is responsible for the sharpening of the jet. In this sense the weakly damped case provides a qualitative representation of the observed upgradient flux of transient eddy momentum into the tropospheric jet stream. The distinct zonal mean responses to the topography in the two cases have important implications for understanding stationary wave nonlinearity.

b. Strongly damped case

In Fig. 2a we show the stationary eddy streamfunction $\overline{\psi}^*$ induced by the topography in the DNS of (1); Fig. 2b shows the associated Plumb wave activity flux and its divergence. The response is highly structured and we can identify three distinct branches of wave activity propagation. First, wave activity diverges away from the topography into a weak convergence region eastward and poleward of the topography. Second, wave activity diverges away from the topography into a strong convergence region eastward and equatorward of the topography, in the vicinity of the critical line defined by the zero contour of zonal wind. This low-latitude branch has a relatively shorter wavelength but greater amplitude. Third, wave activity diverges away from the critical line eastward of 150°E and propagates poleward before bending back equatorward. This part of the wave response evidently deviates from the classical great circle ray passing through the topography that is predicted by linear theory (Hoskins and Karoly 1981).

We use stationary wave modeling to separate linear and nonlinear effects in this solution. In the SD case, $\overline{\zeta' \mathbf{u}'} = 0$, so the sole source of nonlinearity in (2) and (3) is the stationary eddy potential vorticity flux, which can be decomposed into zonally symmetric and zonally asymmetric components. The zonally asymmetric component is the stationary wave nonlinearity referred to in the stationary wave modeling literature (Ting et al. 2001); the zonally symmetric nonlinear term is a momentum flux convergence, which, as discussed in section 3a,

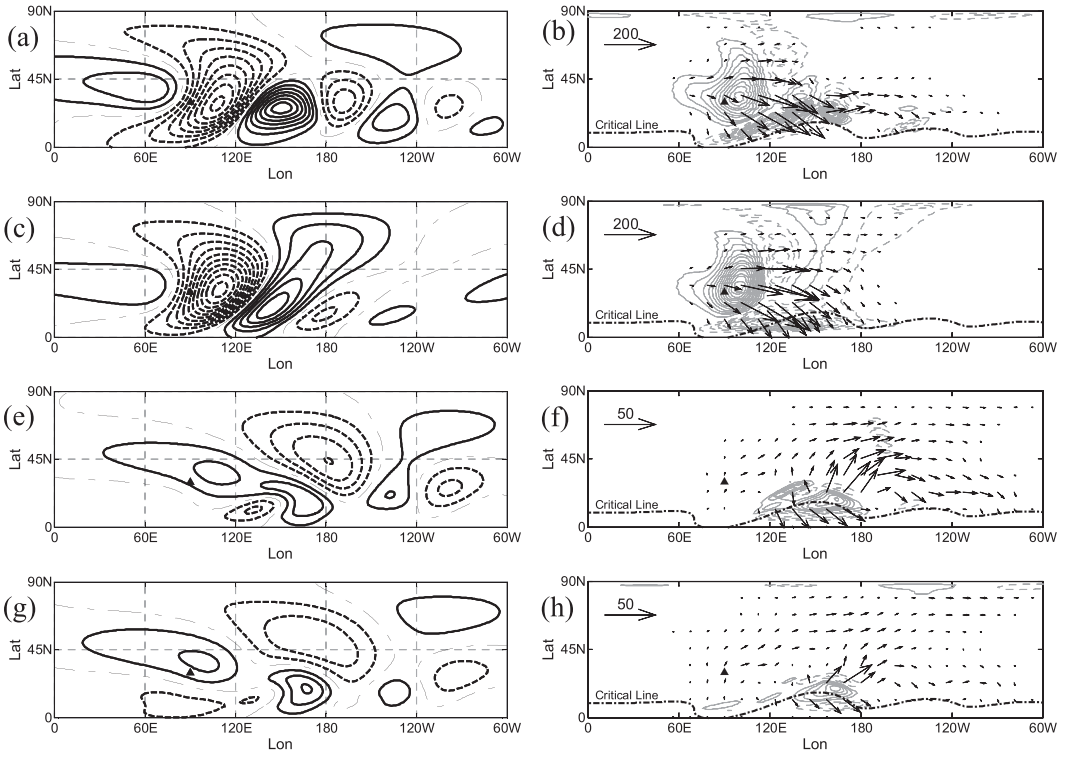

FIG. 2. (left) Streamfunction ($m^2\ s^{-1}$) and (right) associated wave activity flux (arrows, $m^2\ s^{-2}$) and its divergence of the stationary wave responses for $\varepsilon = 2$; the Gaussian mountain is centered at the location of the triangle in each plot. (a),(b) The DNS streamfunction response and its associated wave activity. (c),(d) As in (a),(b), but for the classical linear model. (e),(f) The DNS response minus the linear response in streamfunction and the associated wave activity. (g),(h) Linear model response to zonally asymmetric stationary wave nonlinearity and the associated wave activity. Contour intervals of streamfunction and wave activity divergence are $3 \times 10^6\ m^2\ s^{-1}$ and $1 \times 10^{-5}\ m\ s^{-2}$, respectively. Solid contours are positive; dashed contours are negative; and dashed–dotted contours are zero. The arrows representing wave activity fluxes are 4 times longer in (f) and (h) than in (b) and (d) for graphical display. For this and subsequent plots, the critical lines are indicated by dashed–dotted contours.

drives the zonal mean flow away from U_{ref}. The rest of the zonal mean response comes from the zonal mean of the topography and the hyperdiffusion, which represent smaller terms.

As a test, we can use the linear model, LIN-ANOM, to closely reproduce the nonlinear solution by prescribing $Z = [\bar{\zeta}]_{\text{SD}}$, $U = [\bar{u}]_{\text{SD}}$, and (zonally asymmetric) stationary wave nonlinearity

$$F^* = -\nabla \cdot \left\{ \left(\bar{\zeta}^*_{\text{SD}} + \frac{f_0 h^*}{H} \right) \bar{\mathbf{u}}^*_{\text{SD}} \right\}^* \tag{6}$$

from the DNS solution of (1). Doing so reproduces the DNS solution to a very high precision, with less than 1‰ in relative error between the DNS (1) and LIN-ANOM (4) solutions (not shown).

Next, we can solve the linear model (4) with $Z = \zeta_{\text{ref}}$, $U = U_{\text{ref}}$, $F^* = 0$, and $\tau_E = 5$ days, which represents the classical solution of linear theory. The linear solution (Figs. 2c,d) propagates from the topographic forcing region to the critical layer; has slightly greater amplitude, shorter wavelength, and does not propagate downstream as far as the original solution; and is more consistent with the expected great circle propagation pattern passing through the topography (although we have not checked agreement with the great circle solution in detail).

Nonlinear effects are shown in Fig. 2e, which plots the DNS solution (Fig. 2a) minus the classical linear solution (Fig. 2c); Fig. 2f shows the wave activity associated with this eddy streamfunction pattern (as opposed to the difference in wave activities). We see that the high-latitude branch and the low-latitude branch to the east of 150°E are associated with nonlinear effects. In addition, we see another wave train pattern emanating poleward of the critical line east of 150°W. Thus, the dominant nonlinear effect in this solution is critical layer reflection, which occurs in this highly damped setting through self-advection of stationary wave potential vorticity. Nonlinear reflection of Rossby wave trains is usually characterized by localized overturning PV contours associated

with wave breaking (Brunet and Haynes 1996; Walker and Magnusdottir 2003, and references therein). Weak PV overturning is observed when the topographic forcing is strong (i.e., 2000 and 1000 m), but nonlinear stationary wave reflection still exists with weaker topographic forcing even though the stationary wave does not homogenize the potential vorticity field (not shown because the patterns are similar to those in the 2000-m case except with smaller amplitude). In the discussion, we return to the issue of when critical-layer reflection can be expected to occur.

We can now use the stationary wave model to separately diagnose the stationary wave response in terms of changes to zonally asymmetric forcing terms and of changes to the zonal mean basic state. Although both the zonally asymmetric forcing terms and the zonal mean basic state depend on the stationary wave field, we find that such diagnostics can provide physical insight. In the SD case, we find that it is the stationary wave nonlinearity that is most important: when we calculate the response to F^* from (6) with the zonal mean basic state corresponding to $U_{\rm ref}$, we get a pattern (Figs. 2g,h) that accounts for the main features of Figs. 2e,f; in particular, stationary wave nonlinearity generates the critical layer reflection term. The complementary case, in which the basic state is altered by the stationary eddy forcing and F^* is set to zero, yields only a weak wave response (not shown). This solution is sometimes referred to a ''quasi-linear'' solution (e.g., Davey 1980; Haynes and McIntyre 1987).

c. *Weakly nonlinear asymptotic theory for the SD case*

To better understand stationary wave nonlinearity in the SD case, we develop a weakly nonlinear asymptotic theory that shows how stationary wave nonlinearity arises as part of the rectified effect of the eddy PV flux from the linear solution. In (2) and (3), we see that the topographic forcing comes in as a term proportional to εZ_0; for topography to represent a small perturbation, we require $\varepsilon \ll 1$. We perform a standard asymptotic analysis involving small-parameter expansion in ε, neglecting the hyperviscosity term in (1). We express the variables as asymptotic series in the standard way: $\hat{\zeta} = \hat{\zeta}_0 + \varepsilon\hat{\zeta}_1 + \varepsilon^2\hat{\zeta}_2 + \cdots$ and $\hat{\mathbf{u}} = \hat{\mathbf{u}}_0 + \varepsilon\hat{\mathbf{u}}_1 + \varepsilon^2\hat{\mathbf{u}}_2 + \cdots$, where the variables with a hat are nondimensional. We also assume that the advective and damping time scales are comparable: $\tau_Z \sim \tau_E \sim \zeta^{-1} \sim Z_0^{-1}$. Then to $O(\varepsilon^0 = 1)$, the leading-order vorticity and winds are $\zeta_0 = \zeta_{\rm ref}$, $\mathbf{u}_0 = (U_{\rm ref}, 0)$, and $\mathbf{u}_0^* = 0$, where ζ_0 is the dimensional version of $\hat{\zeta}_0$, $\mathbf{u}_0$ is the dimensional version of $\hat{\mathbf{u}}_0$, and so on. To $O(\varepsilon)$, we have

$$O(\varepsilon):\ [\mathbf{u}_1] = 0, \quad [\zeta_1] = 0,$$
$$U_{\rm ref}\frac{\partial\zeta_1^*}{a\cos\theta\partial\lambda} + v_1^*\frac{\partial}{a\partial\theta}(f + [\zeta_{\rm ref}]) + \frac{1}{\tau}\zeta_1^* = -\frac{f_0U_{\rm ref}}{H}\frac{\partial h^*}{a\cos\theta\partial\lambda},$$

where again all fields and coordinates are understood to be dimensional. The contribution to the zonal mean flow at this order is zero, and the zonally asymmetric flow satisfies the classical linear stationary wave equation. Nonlinear terms come in at $O(\varepsilon^2)$. The dimensional zonal equation is

$$O(\varepsilon^2):\ \nabla\cdot\left[\left(\zeta_1^* + \frac{f_0h^*}{H}\right)\mathbf{u}_1^*\right] = -\frac{1}{\tau}[\zeta_2], \tag{7}$$

showing that the zonally symmetric component at second order is driven by the eddy PV flux associated with the first-order fields (and topography), and the dimensional zonally asymmetric equation is

$$O(\varepsilon^2):\ U_{\rm ref}\frac{\partial\zeta_2^*}{a\cos\theta\partial\lambda} + v_2^*\frac{\partial(f + [\zeta_{\rm ref}])}{a\partial\theta} + \frac{1}{\tau}\zeta_2^* = -\frac{f_0v_1^*}{H}\frac{\partial[h]}{a\partial\theta} - \nabla\cdot\left\{\left(\zeta_1^* + \frac{f_0h^*}{H}\right)\mathbf{u}_1^*\right\}^*, \tag{8}$$

showing that stationary wave nonlinearity, in the sense of Ting and Yu (1998), comes in as the zonally asymmetric component of this eddy PV flux.

In Fig. 3, we test the accuracy of the weakly nonlinear asymptotic solution given by (7) and (8) as the mountain height increases. In Fig. 3a, we show the zonal mean winds predicted by the solution for mountains of various height. In Fig. 3b, we plot the wave solution's Taylor diagram, in which the target point refers to the stationary wave in the DNS minus the stationary wave in the classical linear model (e.g., Fig. 2e for $h_0 = 2000$ m). As the forcing magnitude decreases, the second-order correction approaches this target field, illustrated by a series of arrows in Fig. 3b. The Taylor diagram gives a good measure of how well a linear prognostic theory can estimate the self-nonlinearity of the stationary wave responses to various forcing amplitudes. The solution remains reasonably good as long as $\varepsilon = f_0h_0/Z_0H < \frac{1}{2}$, which corresponds to a 500-m mountain for a depth of 10 km.

In sum, for the SD case, the linear response to isolated topography involves transmission of the wave packet to the critical latitude and absorption of the wave activity there. The nonlinear response involves reflection of the wave activity, and this is captured by the stationary wave nonlinearity, which is the eddy potential vorticity flux here. The zonally symmetric contribution to the solution

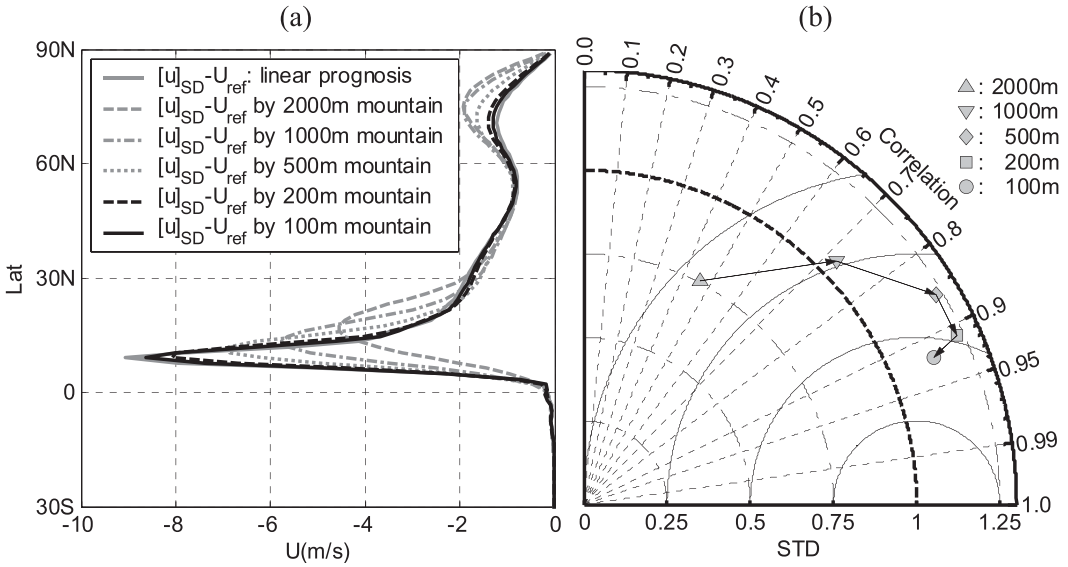

FIG. 3. (a) The zonal-mean zonal wind response (m s^{-1}) for the weakly nonlinear asymptotic theory (7) and for DNS solutions $[u]_{SD} - U_{ref}$ for $\varepsilon = \{0.1, 0.2, 0.5, 1, 2\}$ by $h_0 = \{100, 200, 500, 1000, 2000\}$ m normalized by the reciprocal square of the mountain height. (b) Taylor (2001) diagram comparing the stationary wave response for the weakly nonlinear asymptotic theory (8) to the target field, which is the stationary wave in the DNS minus the stationary wave in the classical linear model (e.g., Fig. 2e for $\varepsilon = 2$), for the cases in (a). In a Taylor diagram, the point 1 along the x axis corresponds to perfect agreement between the solutions, the orientation of the point is related to correlation between the fields (as indicated by the quarter circle labeled ''correlation''), and the distance from the origin indicates amplitude relative to the amplitude of the target field.

is relatively small. Furthermore, we have found that the stationary wave nonlinearity can be reasonably predicted in terms of the eddy vorticity flux from the linear solution. By contrast, we will see several differences in the WD case.

d. Weakly damped case

Our aim in this subsection is to see how transient eddies affect our conclusions about the role of stationary wave nonlinearity of the SD case. We have not extended the weakly nonlinear asymptotic theory of section 3c to this case because there is no well-established statistical closure to describe the transient eddy PV flux. We will thus limit our analysis to the numerical models described in section 2. We recall that in the WD case, as described at the beginning of this section, the transient eddies act to sharpen the jet (see Fig. 1; we also note a zonal wind response seen in the Southern Hemisphere polar region, associated with eddies that propagate across the equator, but this will not be discussed further). The stationary wave streamfunction response in DNS is shown in Fig. 4a. Similarly to the SD case, we see Rossby wave reflection and propagation into multiple branches. The WD stationary wave response has larger amplitude than the SD response and more wave energy propagates farther downstream because of the removal of the damping on waves. But the more fundamental difference in the dynamics is seen when we analyze the interplay between the controlling factors in the solution, as diagnosed by the LIN-ANOM model.

The WD case is more complex than the SD case because we have no predictive theory (closure) for the transient eddy PV fluxes. We introduce a new notation to discuss separately the impacts of transient and stationary eddies. We refer to the stationary nonlinear terms as S and the transient nonlinear terms as T. The linear model solution's dependence on S and T can be written schematically as

$$\psi^* = \mathbf{L}\{U([S], [T]), F^*(S^*, T^*)\},$$

where U depends on the zonal components of the stationary and transient eddy nonlinearity $[S]$ and $[T]$ and F^* depends on the zonally asymmetric component of the stationary and transient eddy forcing S^* and T^*. In the linear calculation, we include the dependence on $[S]$ and $[T]$ by changing the zonal mean basic state to be in balance with these terms, according to the zonal mean equation (2). The classical linear case corresponds to $\mathbf{L}\{U([S] = 0, [T] = 0), F^*(S^* = 0, T^* = 0)\}$; note that $U([S] = 0, [T] = 0)$ corresponds to U_{ref}, apart from hyperdiffusion effects.

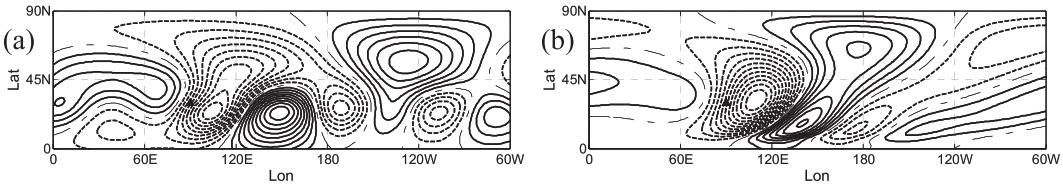

FIG. 4. (a) Streamfunction ($m^2\ s^{-1}$) of the stationary wave responses for $\varepsilon = 2$ for the DNS of the WD case. (b) Streamfunction response ($m^2\ s^{-1}$) for the classical linear model, with $\tau_E = 40$ days. Contouring is as in the corresponding plots in Fig. 2.

To obtain the linear solution from the LIN-ANOM model (4), it is necessary to add a weak damping on the waves to suppress resonant modes, which degrade the solution. Thus, in (4), we set, for example, $\tau_E = 40$ days for $\varepsilon = 2$. The classical linear case is shown in Fig. 4b; the only difference between Figs. 4b and 2c is the reduction of the eddy damping, which serves to enhance the poleward branch and increase the amplitude of the solution. The nonlinearity of the solution, which is the difference between Figs. 4a and 4b, is shown in Fig. 5a, and its corresponding wave activity is shown in Fig. 5b, in which critical layer reflection is primarily visible near 15°N, 150°E.

We find that the individual contributions from the zonally asymmetric nonlinear terms in the operator $\mathbf{L}$ do not, in isolation, well explain the critical layer reflection in the WD case, which is in contrast to the SD case, in which S^* explained much of the nonlinearity. For example, in Figs. 5c,d we show the streamfunction and wave activity for $\mathbf{L}\{U([S] = 0, [T] = 0), F^*(S^* = S^*_{\mathrm{WD}}, T^* = 0)\}$, which includes stationary wave nonlinearity. In contrast to the SD case, the WD S^* alone does not account for critical layer reflection (compare Figs. 5c,d to Figs. 2e,f). The case $\mathbf{L}\{U([S] = 0, [T] = 0), F^*(S^* = 0, T^* = T^*_{\mathrm{WD}})\}$ (Figs. 5g,h), in which only the zonally asymmetric transient eddy nonlinearity is included, provides a solution which is largely of opposite sign to the previous case. We find that the S^* and T^* components in these cases are generally of opposite sign (not shown), which is consistent with our previous finding that $[S]$ and $[T]$ acted in opposite senses on the zonal jet (section 3a).

After some trial and error experimentation, we have found two ways of producing the key nonlinear effects. One way, corresponding to the operator $\mathbf{L}\{U([S] = [S]_{\mathrm{WD}}, [T] = 0), F^*(S^* = S^*_{\mathrm{WD}}, T^* = 0)\}$ (Figs. 5i,j), is to include both the zonally symmetric and zonally asymmetric stationary nonlinear terms. This case produces significant reflection near 15°N, 150°E and the overall feature of the wave activity pattern is fairly consistent with that in Fig. 5b. The other way is to include the jet sharpening effect of the transient eddy forcing, using $\mathbf{L}\{U([S] = 0, [T] = [T]_{\mathrm{WD}}), F^*(S^* = 0, T^* = 0)\}$ (Figs. 5k,l). This change in the basic state alone can induce considerable reflection wave energy back to midlatitudes, but the location of the reflection is much broader than that in Fig. 5b and the pattern around the reflection area in the streamfunction plot (Fig. 5k) is not similar to that in Fig. 5a. This effect is diminished when the zonal mean adjustment to the stationary eddy forcing is reintroduced—$\mathbf{L}\{U([S] = [S]_{\mathrm{WD}}, [T] = [T]_{\mathrm{WD}}), F^*(S^* = 0, T^* = 0)\}$, Figs. 5e,f—again because of the opposite impact of the stationary and transient eddy forcings on the zonal mean jet.

Thus, critical layer reflection downstream from the topography can be induced by the combination of stationary wave nonlinearity and its impact on the zonal mean basic state. The zonal mean basic state response to transients is able to induce pronounced reflection but does not put the reflection in the right location. There is no evidence indicating the involvement of the time mean zonally varying component of transient eddy forcing in the reflection in our simulation.

e. Nonlinear stationary wave model

One of our applied goals in this study is to test the Ting and Yu (1998) and Held et al. (2002) nonlinear stationary wave modeling approach in the presence of transient eddy forcing. In the NONLIN-ANOM model (5), the zonal flow and T^* are prescribed, but the stationary nonlinearity is calculated internally instead of being prescribed. The flow is stabilized by τ_E. A linear damping is still required to suppress the transients generated internally, while an absolutely steady flow is achieved only with an unrealistically strong damping. The magnitude of the damping is chosen as a tradeoff between the need to suppress transients and the need to maintain a good-quality solution relative to the DNS. The 40-day damping used in the linear WD calculation appears suitable for a good solution to (5); it produces transient eddy fluxes that are an order of magnitude smaller than those found in the WD DNS. This technique is similar to the treatment in Held et al. (2002), in which weak transients are present that are not strong enough to significantly modify the solution.

In Fig. 6, we show a Taylor diagram comparing the LIN-ANOM model and the NONLIN-ANOM model in the WD case. The plotting symbols are grouped according

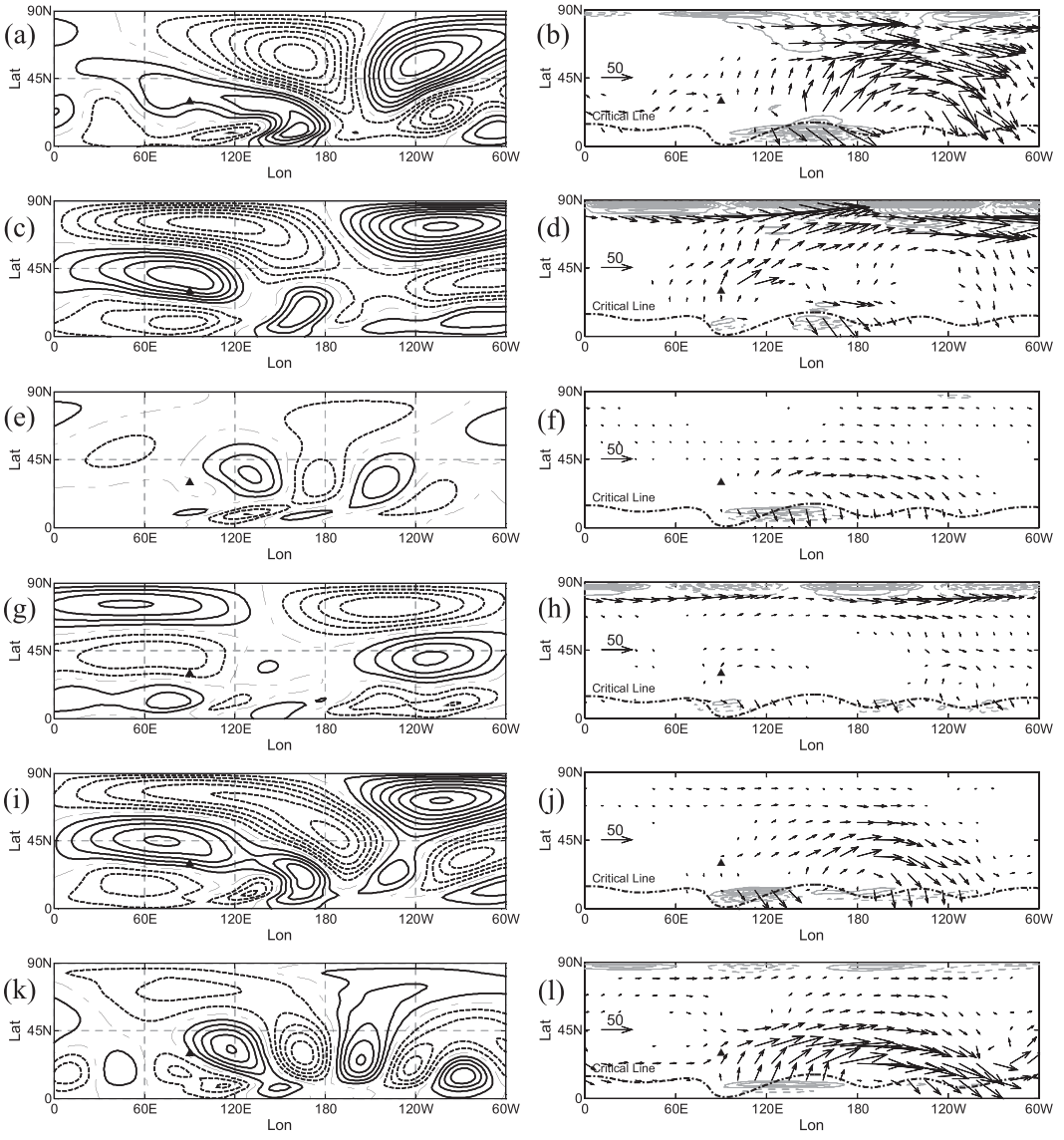

FIG. 5. As in Fig. 2, but for the WD case. (a),(b) DNS minus the classical linear response (i.e., Fig. 4a minus Fig. 4b) and the associated wave activity. Following this are plotted the responses diagnosed from the linear model to (c),(d) zonally asymmetric stationary eddy forcing, (e),(f) zonally symmetric transient and stationary eddy forcing, (g),(h) zonally asymmetric transient eddy forcing, (i),(j) combined zonally symmetric and zonally asymmetric stationary eddy forcing, and (k),(l) zonally symmetric transient eddy forcing.

to whether stationary wave nonlinearity is neglected $\{F^*(S^*) = 0$, gray symbols$\}$, prescribed from the WD DNS in the LIN-ANOM model $\{F^*(S^*) = F^*(S^*_{\mathrm{WD}})\}$, black symbols], or predicted with the NONLIN-ANOM model (white symbols). The sensitivity of neglecting, prescribing, or predicting stationary wave nonlinearity to the presence of the remaining nonlinear effects is explored in the figure. In all cases, neglecting stationary wave nonlinearity seriously degrades the agreement with the DNS. We see that the NONLIN-ANOM model reproduces the effect of prescribed stationary wave nonlinearity $F^*(S^*)$ in the LIN-ANOM model for various combinations of forcings fairly well, in terms of both correlation and amplitude. The worst performance comes for the case in which the zonally asymmetric transient eddy forcing is prescribed without any change to the zonal mean (white triangle). Overall, this comparison supports the validity of the nonlinear stationary wave modeling technique, confirms the necessity of including the stationary wave nonlinearity in stationary wave modeling, and highlights the importance of zonal mean adjustment. All the nonlinear model integrations are

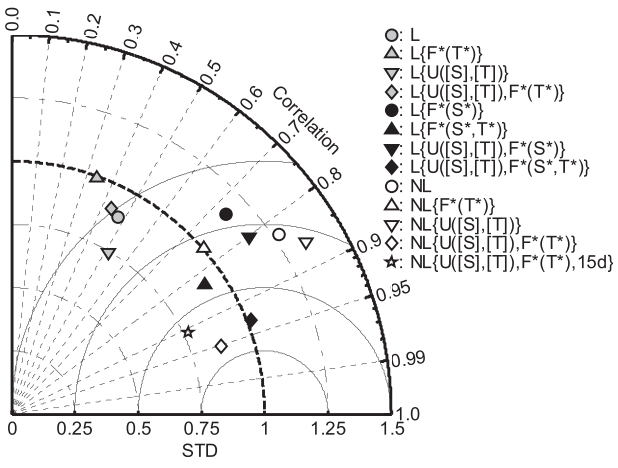

FIG. 6. Taylor diagrams of the linear and nonlinear stationary wave solutions compared with the target stationary wave solution in the DNS of the WD case. Shown are the responses with $U = U_{\text{ref}}$ and no transient eddy forcing (circles), with zonally asymmetric transient eddy forcing (upward pointing triangles), with zonally symmetric stationary plus transient eddy forcing (downward pointing triangles), and with zonally symmetric stationary plus transient eddy forcing and zonally asymmetric transient eddy forcing (diamonds). The star represents the latter case for the nonlinear model with damping increased to completely suppress transient eddies. The black symbols represent the linear model with the prescribed stationary nonlinearity forcing, and the gray ones are without the stationary wave nonlinearity forcing. All runs have $\tau_E = 40$ days, except for the star case which has $\tau_E = 15$ days.

with $\tau_E = 40$ days, except for the one indicated by a star symbol, which achieves complete suppression of the transient eddies with $\tau_E = 15$ days.

4. Summary and discussion

We have used simple barotropic QG dynamics to improve our understanding of stationary wave nonlinearity in barotropic dynamics. We have shown that stationary wave nonlinearity in our model is primarily manifested as critical layer reflection in the absence and presence of transient eddies. In the weakly damped case with transient eddies, a combination of adjustments to the zonal mean and stationary wave nonlinearity is required to accurately reproduce the pattern of critical layer reflection in the DNS solution. Although including the zonal mean adjustment to the transient eddy forcing also results in reflection (Figs. 5k,l), presumably through a change in the refractive properties of the basic state (Karoly 1983; Hoskins and Ambrizzi 1993), the spatial distribution of the wave activity associated with this effect is not fully consistent with the reflection pattern of the DNS solution.

How general are the effects we have described here? In the cases shown here and additional cases we have analyzed, we find local stationary wave activity reflection where stationary wave amplitudes are large enough to induce localized easterlies and weak PV gradients. In fact, we see such reflection even in cases where the zonal mean zonal wind is westerly at all latitudes (not shown). This is similar to what Waugh et al. (1994) saw for total (stationary plus transient) eddy wave activity fluxes.

We also used a weakly nonlinear asymptotic theory to physically interpret stationary wave nonlinearity in the SD case. We find that to leading order, stationary wave nonlinearity represents the PV flux associated with the linear response in the SD case. This theory not only matches the nonlinear solution in the small forcing limit but also expresses the ability to prognose a large portion of both zonally symmetric and asymmetric components of the nonlinear response to finite size forcing. An improved version of this approach might be extended to a multiple stage method to prognose the stationary wave response to an imposed forcing that includes a zonal flow adjustment to stationary wave forcing. This might potentially provide an advance over standard approaches in which the zonal mean is fixed (e.g., Valdes and Hoskins 1991) and avoid reported sensitivities to the zonal mean basic state used (Ting and Sardeshmukh 1993). It should be remembered, however, that in the absence of a statistical closure for transient eddy fluxes, this theory does not extend to the WD case. The fact that stationary and transient eddy effects oppose each other in this simple system suggests that care needs to be taken with such an approach in both barotropic and baroclinic systems.

The Ting–Yu nonlinear technique of stationary wave modeling is now being employed to calculate stationary wave nonlinearity in observations and climate simulations. We have attempted to quantify its performance and found that the Ting–Yu approach works best when zonal mean adjustments are included and eddy damping is used that does not entirely remove transients from the solution. Our results suggest that in the presence of transient eddies, such as baroclinic eddies in the troposphere or the transient planetary waves of the stratosphere, stationary wave models will be qualitatively more accurate if the zonal mean flow adjustment is explicitly accounted for. Construction of such models is a topic of ongoing work, as well as the generalization of the results of this study to the baroclinic case. There certainly exist other types of stationary wave nonlinearity in more complicated systems, such as the nonlinear interaction between topography and diabatic heating forced stationary waves (see review in Held et al. 2002), which are subjects of future investigation.

Acknowledgments. We gratefully acknowledge the support of the National Sciences and Engineering Research Council of Canada and the Canadian Foundation

for Climate and Atmospheric Sciences. We also thank the anonymous reviews for their helpful comments.

REFERENCES

Brandefelt, J., and H. Körnich, 2008: Northern Hemisphere stationary waves in future climate projections. *J. Climate,* **21,** 6341–6353.

Brunet, G., and P. H. Haynes, 1996: Low-latitude reflection of Rossby wave trains. *J. Atmos. Sci.,* **53,** 482–496.

Chang, E. K. M., 2009: Diabatic and orographic forcing of northern winter stationary waves and storm tracks. *J. Climate,* **22,** 670–688.

Davey, M. K., 1980: A quasi-linear theory for rotating flow over topography. I. Steady beta-plane channel. *J. Fluid Mech.,* **99,** 267–292.

Haynes, P. H., and M. E. McIntyre, 1987: On the representation of Rossby wave critical layers and wave breaking in zonally truncated models. *J. Atmos. Sci.,* **44,** 2359–2382.

——, ——, T. G. Shepherd, C. J. Marks, and K. P. Shine, 1991: On the ''downward control'' of extratropical diabatic circulations by eddy-induced mean zonal forces *J. Atmos. Sci.,* **48,** 651–678.

Held, I. M., 1985: Pseudomomentum and the orthogonality of modes in shear flows. *J. Atmos. Sci.,* **42,** 2280–2288.

——, and P. J. Phillips, 1987: Linear and nonlinear barotropic decay on the sphere. *J. Atmos. Sci.,* **44,** 200–207.

——, M. F. Ting, and H. L. Wang, 2002: Northern winter stationary waves: Theory and modeling. *J. Climate,* **15,** 2125–2144.

Hoskins, B. J., and D. J. Karoly, 1981: The steady linear response of a spherical atmosphere to thermal and orographic forcing. *J. Atmos. Sci.,* **38,** 1179–1196.

——, and T. Ambrizzi, 1993: Rossby wave propagation on a realistic longitudinally varying flow. *J. Atmos. Sci.,* **50,** 1661–1671.

Jin, F., and B. J. Hoskins, 1995: The direct response to tropical heating in a baroclinic atmosphere. *J. Atmos. Sci.,* **52,** 307–319.

Joseph, R., M. F. Ting, and P. J. Kushner, 2004: The global stationary wave response to climate change in a coupled GCM. *J. Climate,* **17,** 540–556.

Karoly, D. J., 1983: Rossby wave propagation in a barotropic atmosphere. *Dyn. Atmos. Oceans,* **7,** 111–125.

Nigam, S., and I. Held, 1983: The influence of a critical latitude on topographically forced stationary waves in a barotropic model. *J. Atmos. Sci.,* **40,** 2610–2622.

Plumb, R. A., 1985: On the three-dimensional propagation of stationary waves. *J. Atmos. Sci.,* **42,** 217–229.

Ringler, T. D., and K. H. Cook, 1997: Factors controlling nonlinearity in mechanically forced stationary waves over orography. *J. Atmos. Sci.,* **54,** 2612–2629.

Taylor, K. E., 2001: Summarizing multiple aspects of model performance in a single diagram. *J. Geophys. Res.,* **106,** 7183–7192.

Ting, M., 1994: Maintenance of northern summer stationary waves in a GCM. *J. Atmos. Sci.,* **51,** 3286–3308.

——, and P. D. Sardeshmukh, 1993: Factors determining the extratropical response to equatorial diabatic heating anomalies. *J. Atmos. Sci.,* **50,** 907–918.

——, and L. H. Yu, 1998: Steady response to tropical heating in wavy linear and nonlinear baroclinic models. *J. Atmos. Sci.,* **55,** 3565–3582.

——, H. L. Wang, and L. H. Yu, 2001: Nonlinear stationary wave maintenance and seasonal cycle in the GFDL R30 GCM. *J. Atmos. Sci.,* **58,** 2331–2354.

Valdes, P. J., and B. J. Hoskins, 1991: Nonlinear orographically forced planetary waves. *J. Atmos. Sci.,* **48,** 2089–2106.

Vallis, G. K., 2006: *Atmospheric and Oceanic Fluid Dynamics*. Cambridge University Press, 745 pp.

Walker, C. C., and G. Magnusdottir, 2003: Nonlinear planetary wave reflection in an atmospheric GCM. *J. Atmos. Sci.,* **60,** 279–286.

Waugh, D. W., R. A. Plumb, and L. M. Polvani, 1994: Nonlinear, barotropic response to a localized topographic forcing: Formation of a ''tropical surf zone'' and its effect on interhemispheric propagation *J. Atmos. Sci.,* **51,** 1401–1416.